

1

2

Geophysical Research Letters

3

Supporting Information for

4

Jupiter's X-ray and UV Dark Polar Region

5

W. R. Dunn^{1,2}, D. M. Weigt^{3,4}, D. Grodent⁵, Z. H. Yao^{6,7}, D. May⁸, K. Feigelman⁸, B. Sipos⁸, D. Fleming⁸, S. McEntee^{4,9}, B. Bonfond⁵, G. R. Gladstone^{10,11}, R. E. Johnson¹², C. M. Jackman⁹, R. L. Guo¹³, G. Branduardi-Raymont^{1,2}, A. D. Wibisono^{1,2}, R. P. Kraft¹⁴, J. D. Nichols¹⁵, L. C. Ray¹⁶

6

7

8

¹Mullard Space Science Laboratory, University College London, Dorking, UK.

9

²The Centre for Planetary Science at UCL/Birkbeck, Gower Street, London WC1E 6BT, UK.

10

³School of Physics and Astronomy, University of Southampton, Southampton, SO17 1BJ, UK

11

⁴School of Physics, Trinity College Dublin, Dublin, Ireland

12

⁵Laboratoire de Physique Atmosphérique et Planétaire, STAR institute, Université de Liège, Liège, Belgium.

13

14

⁶Key Laboratory of Earth and Planetary Physics, Institute of Geology and Geophysics, Chinese Academy of Sciences, Beijing, China.

15

16

⁷College of Earth and Planetary Sciences, University of Chinese Academy of Sciences, Beijing, China.

17

18

⁸Department of Science, St. Gilgen International School, St. Gilgen, Austria

19

⁹School of Cosmic Physics, DIAS Dunsink Observatory, Dublin Institute for Advanced Studies, Dublin 15, Dublin, Ireland

20

21

¹⁰Space Science and Engineering Division, Southwest Research Institute, San Antonio, TX, USA

22

¹¹Department of Physics and Astronomy, University of Texas at San Antonio, San Antonio, TX, USA

23

24

¹²Department of Physics, Aberystwyth University, Aberystwyth, Ceredigion, SY23 3FL

25

¹³Laboratory of Optical Astronomy and Solar-Terrestrial Environment, Institute of Space Sciences, School of Space Science and Physics, Shandong University, Weihai, Shandong, China.

26

27

¹⁴Harvard-Smithsonian Center for Astrophysics, Smithsonian Astrophysical Observatory, Cambridge, MA, USA

28

29

¹⁵Department of Physics and Astronomy, University of Leicester, Leicester, LE1 7RH, UK

30

¹⁶Department of Physics, Lancaster University, Lancaster, UK

31

32

Contents of this file

33

Text S1

34

Figures S1

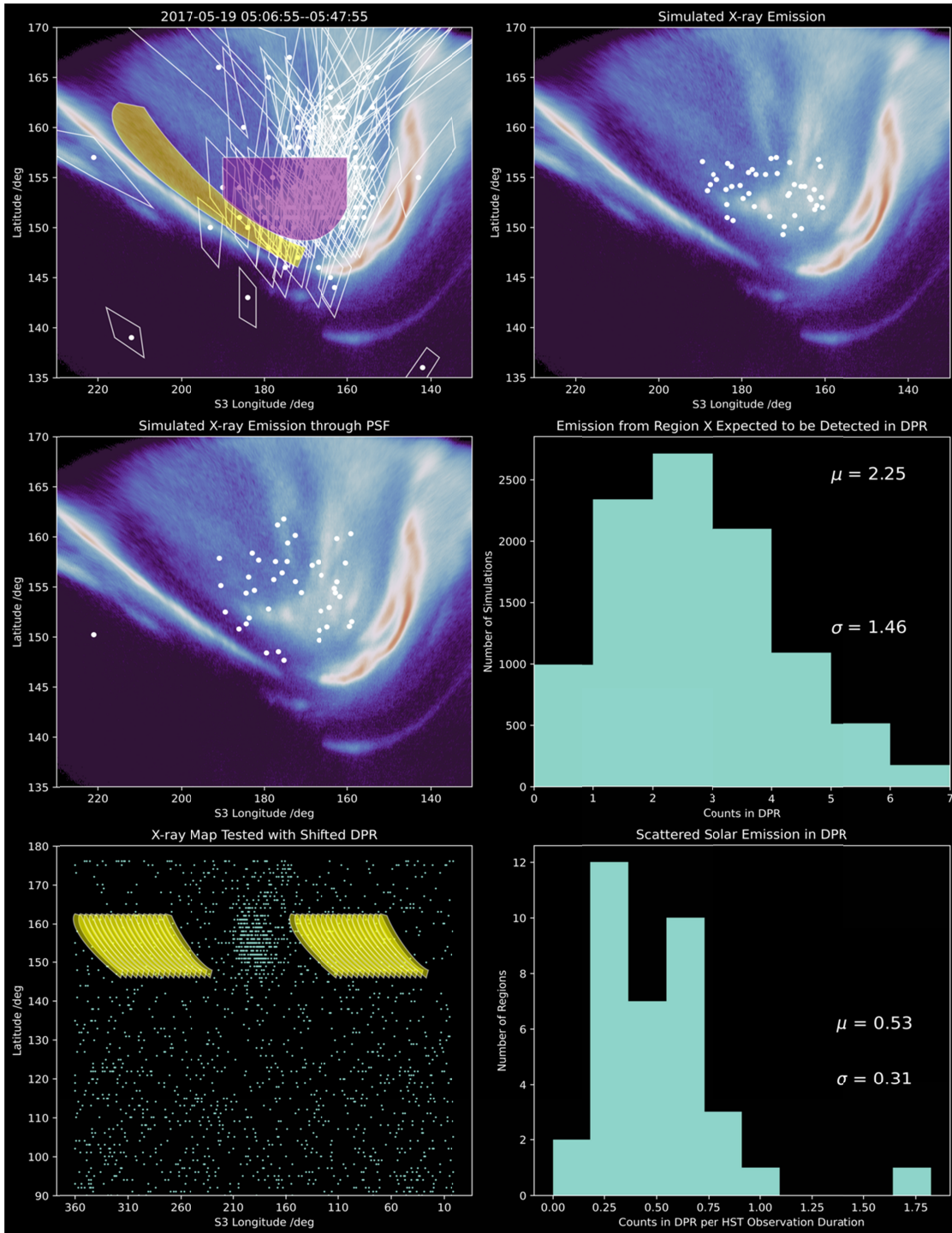
35

Tables S1

36 **Text S1.**

37 To explore the difference between a uniformly distributed probability of X-ray emission
38 from region X (i.e. each latitude-longitude location in region X has an equal probability of
39 being the source of the simulated X-ray) and the UV-driven X-ray probability distribution
40 outlined in the main text, we ran 100,000 simulations with a uniform distribution for each
41 observation. An example simulation run is shown in Figure S1, with the resulting counts for all
42 observations in Table S1. For all observations the mean from the UV distribution is within 1
43 standard deviation of the mean for a uniform distribution.

44
45 Alongside this, Table S1 provides the number of observed counts per square degree
46 within region X and the DPR. Then, using this value, the table provides an expected counts in
47 region X if it produced the same number of photons per square degree as the DPR ('if the DPR
48 was region X-like'). Similarly, the table also provides an expected number of counts in the DPR
49 if it produced the same number of counts per square degree as Region X ('if Region X was
50 DPR-like'). This accounts for the difference in spatial size of each region from observation to
51 observation and highlights the discrepancy in X-rays detected in each of the two regions.



56
 57 **Figure S1.** Same as Figure 2 in the main text, but using a uniform probability to determine the
 58 longitude-latitude location from which an X-ray is generated in region X (purple region in the top
 59 left panel), rather than deriving the probability distribution from the UV brightness in region X.

57

CXO-HST Joint Observation	DPR Counts	Region X Counts	DPR Photons / sq deg	Region X Photons / sq deg	Expected DPR counts if region X- like	Expected region X counts if DPR-like	Expected Region X X- rays Detected in DPR if Uniformly Distributed
YYYY-MM- DD T hh:mm- hh:mm							
2016-05-24 T17:45- 18:29	0	26	0	0.1	13	0	1.6±1.2
2016-05-24 T20:56- 21:40	3	23	0.03	0.1	16	4	0.7±0.8
2016-06-01 T14:57- 15:41	4	12	0.009	0.04	18	3	1.4±0.4
2016-06-01 T18:08- 18:52	3	9	0.01	0.02	6	5	0.6±0.8
2017-02-02 T16:58- 17:38	1	11	0.01	0.04	3	4	0.4±0.6
2017-03-27 T08:41- 09:21	0	7	0	0.02	2	0	0.1±0.3
2017-05-19 T05:06- 05:46	4	39	0.03	0.2	29	5	2.3±1.4
2017-05-19 T06:42- 07:22	0	24	0	0.08	9	0	1±1
2018-04-01 T10:38- 10:56	0	12	0	0.06	9	0	0.7±0.8
2018-05-24 T09:39- 10:09	1	15	0.004	0.05	15	1	0.7±0.8
2018-09-07 T05:10- 05:50	1	1	0.007	0.004	1	2	0.1±0.3

2019-07-15 T14:43- 15:21	3	17	0.01	0.06	13	4	2.1±1.4
2019-07-15 T16:16- 16:54	3	16	0.02	0.07	10	5	0.8±0.9
2019-07-16 T11:20- 11:58	3	24	0.02	0.11	16	4	2±1

57 **Table S1.** X-ray counts from the DPR for the time intervals shown in the first column. Northern
58 aurora X-ray photons are only included from the time window in the first column. The columns
59 compare the number of X-ray photons detected in the DPR and region X, the number of photons
60 per square degree in the DPR and region X. From these values, we calculated the expected number
61 of detected photons in the DPR if it was region X like and in region X if it was DPR-like. This
62 highlights the clear difference in photon distribution between the two regions. The final column
63 shows the number of photons from the active and swirl region that are expected to be detected in
64 the DPR because of uncertainties in the photon spatial location (see e.g. Figure 3C and D) as
65 mean±standard deviation from 100,000 simulation runs, based on a simulated uniform probability
66 across region X.